

PUBLICATIONS

Publication during Ph.D.:

1. Engineering Degrons of Yeast Ornithine Decarboxylase as Vehicles for Efficient Targeted Protein Degradation
Rushikesh G. Joshi, Swapnali Kulkarni, C. Ratna Prabha*
Biochimica et Biophysica Acta (BBA) - General Subjects
Volume 1850, Issue 12, December 2015, Pages 2452–2463
2. Combination of degrons from yeast and mammalian ornithine decarboxylase enzymes for effective targeted degradation of proteins
Rushikesh G. Joshi, C. Ratna Prabha*
(Manuscript under preparation)
3. Coevolution of Ornithine decarboxylase and antizyme
Rushikesh G. Joshi, Sneha Shah, P. V. Balaji*, C. Ratna Prabha*
(Manuscript under preparation)

Other Publications :

1. Synthesis, spectroscopic characterization and DNA nuclease activity of Cu(II) complexes derived from pyrazolone based NSO-donor Schiff base ligands.
Komal M. Vyas, **Rushikesh G. Joshi**, R.N. Jadeja, C. Ratna Prabha, Vivek K. Gupta
Spectrochimica Acta Part A 84 (2011) 256– 268
2. Syntheses, characterization and molecular structures of calcium(II) and copper(II) complexes bearing O²-chelate ligands: DNA binding, DNA cleavage and anti-microbial study
R.N. Jadeja, Komal M. Vyas, Vivek K. Gupta, **Rushikesh G. Joshi**, C. Ratna Prabha
Polyhedron, 31 (2012) 767–778
3. Superiority of herbal and natural antioxidants mix therapy over their individual application in methylmercury induced stressed chick: Ashwagandha, Vitamin E and Glutathione combinations.
Sood, P. P., Gupte, K., **Joshi, R.**, Vekariya, V., Vekaria, P., Delvadiya, C., Ankola, P., Barchha, S., Manvar, R., Joshi, K. K. and Shah, A.
Journal of Cell and Tissue Research, Vol. 10(1): 2049-2058 (2010)
4. Superiority of herbal and natural antioxidants mix therapy over their individual application in methylmercury induced stressed chick: Curcumin, Vitamin B complex and Glutathione combinations.
Sood, P. P., **Joshi, R.**, Gupte, K., Vekariya, V., Vekaria, P., Delvadiya, C., Ankola, P., Barchha, S., Manvar, R., Kundu, R. S., Joshi, K. K. and Shah, A.
Journal of Cell and Tissue Research, Vol. 9(2) 1803-1810 (2009).



Engineering degrons of yeast ornithine decarboxylase as vehicles for efficient targeted protein degradation[☆]



Rushikesh G. Joshi, Swapnali Kulkarni, C. Ratna Prabha^{*}

Department of Biochemistry, Faculty of Science, The Maharaja Sayajirao University of Baroda, Vadodara 390002, India

ARTICLE INFO

Article history:

Received 21 April 2015

Received in revised form 3 September 2015

Accepted 8 September 2015

Available online 9 September 2015

Keywords:

Ornithine decarboxylase

Degron

Degradation determinant signal

Structure of degron

Function of degron

CD spectrum

ABSTRACT

Background: Ornithine decarboxylase (ODC), which catalyzes the first step of polyamine biosynthesis, undergoes rapid targeted degradation (TPD) with the help of its two degron sequences, namely the N-terminal 50 residues (N50) and α/β domain (α/β) housing antizyme binding element (AzBE), in response to increased polyamine levels. Antizyme binds to AzBE of ODC and delivers it to proteasome for degradation. Entire ODC was used as a tag to demonstrate TPD of chimeric proteins.

Methods: Here we fashioned three peptide sequences from yeast ODC to test their capability to act as degrons, namely N50, α/β and $N\alpha/\beta$ (a combination of N50 and α/β), and monitored their degradation potentials in chimeric proteins. We have examined the correlation between degradation potentials and structural integrity of the peptides, to find mechanistic explanations.

Results: $N\alpha/\beta$ with two signals in tandem is a better degron, under the regulation of antizyme. N50 like N44 reported earlier could drive chimeric proteins to degradation, while α/β could not act as an independent degron. Strong correlation was observed between functional efficacy of the peptides and their structural integrity. N50, which was believed to be unstructured, displayed propensity for helical conformation. $N\alpha/\beta$ exhibited optimal structure, while α/β failed to adopt native like conformation.

Conclusions and general significance: Functional efficacy of the degron $N\alpha/\beta$ is a consequence of its structural integrity. $N\alpha/\beta$ and N50 could target chimeric proteins to degradation. However, α/β failed in the quest. $N\alpha/\beta$, regulated by antizyme, is better suited than N50 for TPD to understand the function of novel proteins.

© 2015 Elsevier B.V. All rights reserved.

1. Introduction

Polyamines are ubiquitous molecules, which bind to nucleic acids, proteins and nucleotide triphosphates, participating in the regulation of cell growth, division and physiology [1–3]. Polyamines are known to stimulate the synthesis of some proteins and determine the assembly and stability of ribosomal subunits in bacteria [4,5] and eukaryotes [6,7] as well. The first and the rate determining step of polyamine biosynthesis is catalyzed by ornithine decarboxylase (ODC) [3]. In eukaryotes the protein is approximately 450 residues long and exists as a homodimer [8]. Homodimer of ODC is enzymatically active and symmetrical, formed as a result of head to tail interaction of the subunits resembling the ‘Yin–Yang’ formation. The active site of ODC is located in the interface of two subunits. The marginally stable dimer of ODC is in dynamic equilibrium with the monomer. This relatively short lived protein [9] undergoes

targeted degradation by 26S proteasomes [10], as a consequence of rise in polyamine levels [11]. However, ODC does not undergo ubiquitination prior to degradation [12–15]. Instead another protein antizyme (OAz1) recognizes a sequence in the monomer of ODC known as antizyme binding element (AzBE) and binds it noncovalently [16]. The antizyme bound to ODC subsequently interacts with regulatory 19S particle of proteasome and delivers ODC for degradation. Antizyme mediated degradation of ODC is under tight regulation dictated by polyamine concentrations. The mRNA of antizyme has two partially overlapping reading frames and the first ORF has a stop codon where the translation is terminated under conditions of polyamine deficit. Under conditions of polyamine sufficiency the ribosome undergoes +1 frameshift just before encountering the stop codon of first ORF and continues to produce a full length antizyme [17,18]. Subsequent decrease in polyamine concentration leads to degradation of antizyme by proteasomes in ubiquitin dependent manner [19,20].

X-ray crystallographic structures of ODC from mouse and human revealed that the enzyme has two domains in its structure [21,22]. The N-terminal of ODC has α/β barrel domain formed by 9 α helices and 8 β -strands arranged in a TIM β -barrel like structure and the C-terminal has a β -sheet domain. On the other hand, structure of yeast ODC (yODC) has not been resolved using NMR spectroscopy or

Abbreviations: ODC, ornithine decarboxylase; AzBE, antizyme binding element; yEGFP, yeast enhanced green fluorescent protein; TFE, 2,2,2-trifluoroethanol.

[☆] This work was supported by a major research project grant (no. BT/PR939/BRB/10/553/2007) awarded to C. Ratna Prabha from Department of Biotechnology, Ministry of Science and Technology, Government of India.

^{*} Corresponding author.

E-mail address: chivukula_r@yahoo.com (C. Ratna Prabha).

X-ray crystallography. Yeast ODC and mammalian ODC (mODC) share 40% sequence homology [23]. However, in yeast ODC there is an extension of 50 amino acid residues in the N-terminal and in the mammalian ODC the C-terminal has a tail of 37 residues with extended structure, which do not have an equivalent in the other protein. The C-terminal tail of mammalian ODC inserts the protein into the proteasomal portal for degradation [24]. Removal of this region from mouse ODC resulted in bringing down the degradation rate [25,26]. In the C-terminal of mammalian ODC there is another degradation determinant signal, namely the highly conserved cysteine residue Cys441. Substitution of Cys441 by alanine, serine or tryptophan made the protein more stable [25–27]. Further, deletion of the C-terminal five amino acid residues from mODC affected the rate of its degradation drastically [25]. The degradation signals of mODC existing in the C-terminal of the enzyme can be recognized by yeast proteasomes [26]. Prior to these studies, Descenzo and Minocha reported in 1993 that expression of cDNA either encoding full-length mODC or truncated form of mODC sans its C-terminal 37 residues led to increase in the levels of polyamines in tobacco plant [28].

Every protein in nature has certain sequences and/or structural features in its design which determine its function, regulation and longevity. Once a protein serves the function it is targeted for degradation with the help of degradation signals or degrons present in its sequence. The process of 'targeted protein degradation' (TPD) seen in nature is increasingly adopted as an effective strategy to bring about rapid degradation of a specific protein with temporal and spatial control [29]. TPD is used as a tool to understand the functions of unknown proteins and can potentially be extended to the removal of pathogenic proteins in certain diseases as a new line of treatment. Initially, it was observed that the nature of N-terminal residue determines the half-life of a protein. N-terminal residues of several proteins were changed to alter their half-lives [30]. Presence of PEST sequences in some proteins has been shown to be cause for their rapid degradation [31]. Full length ODC and the 'degradation determinant signals' or 'degrons' of ODC, were employed as vehicles for targeted protein degradation. Appending C-terminal tail of mODC containing PEST sequence to dihydrofolate reductase resulted in accelerating the rate of its degradation [32]. Besides, removal of the C-terminal from mODC stabilized the protein. Jungbluth and co-workers (2010) combined the above two methods in a path breaking study [33]. They made a bidirectional degron GFP-cODC-Tdeg-F-RFP, by introducing C-terminal degron of mODC at the C-terminal of GFP (green fluorescent protein) and the TEV protease recognition element Tdeg between GFP and RFP (red fluorescent protein). The N-terminal residue of RFP in the construct has destabilizing amino acid phenylalanine (F) and hence it was indicated as F-RFP. To start with, the chimeric protein GFP-Tdeg-F-RFP carried two degrons, which were inaccessible for degradation. Both C-terminal and N-terminal degrons would be exposed only after cleavage of the chimeric construct by inducible TEV protease at the Tdeg site. As a consequence, GFP would be targeted by the exposed C-terminal of mODC to proteasomes for degradation. RFP on the other hand would be targeted to proteasomes through N-end rule dependent polyubiquitination. In another brilliant design, photosensitive LOV2 (light oxygen voltage 2) domain of phototropin was employed as a light sensitive switch [34]. LOV2 was fused to 23 residues long degron resembling C-terminus of mODC. LOV2 has a helical region in its structure which undergoes unfolding upon irradiation with blue light exposing the C-terminus of mODC. Light regulated depletion of chimeric fusion of RFP with this photosensitive degron was demonstrated in yeast system. Most of the strategies described above exploited the degradation potential of C-terminal degron of mODC. Efforts are underway to develop other methods for targeted protein degradation with better temporal and spatial regulation.

Earlier targeted protein degradation was demonstrated successfully using chimeric constructs of human ODC grafted on protein interacting domains [35]. Two main shortcomings encountered with the use of full

length ODC are its enormous size and elevated enzyme activity due to overexpression of the protein. Keeping the degrons intact and pruning ODC to minimal size, was seen by us as the most effective alternative for redesigning ODC into an efficient vehicle for targeted protein degradation. In order to test this hypothesis we have chosen three peptide sequences representing the degrons of full length yeast ODC (yODC): (i) first 50 residues of the N-terminus (N50), (ii) the α/β domain and (iii) the two sequences kept in tandem i.e., N α/β (Fig. 1A). While this work was in progress, Godderz et al. (2011) reported that the N-terminal 44 residues of ODC (ODS) can act as a transplantable degron [36]. Our results establish that N50 like ODS can drive the chimeric proteins to degradation. N α/β with two signals acting in tandem is a better degron. Its activity can effectively be regulated by modulating the levels of antizyme (OAZ1). However, α/β failed to serve the purpose. Further, our results establish unambiguous correlation between the functional efficacy of the peptides and their structure. N-terminal region of ODC encompassing the N50 sequence was believed to be unstructured [36]. In the present study we observed that it has a propensity for helical conformation. Modeling studies indicated interactions between N50 and α/β domain in N α/β peptide. N α/β folded to form optimal secondary and tertiary structure, while α/β failed to take up native like conformation, displaying excessive β -sheet character.

2. Materials and methods

2.1. Strains and plasmids

The strains of *Saccharomyces cerevisiae* used in the present work are Y05034 (*MATa his3 Δ 1 leu2 Δ 0 met15 Δ 0 ura3 Δ 0 spe1::KANMX*), a derivative of BY4741 and Y651 (*Mat_ his3 leu2 lys2 ura3 oaz1::KANMX*). Yeast expression vector pUG35 expressing yEGFP gene under *ADH* promoter was used for engineering yEGFP-degron fusions. Conditions used for bacterial and yeast cultures were as described previously [37, 38]. *S. cerevisiae* strains Y05034 and Y651 expressing yEGFP and degron-yEGFP fusion proteins from plasmid pUG35 were grown in fresh synthetic dextrose (SD) medium under selection pressure. The strains Y05034 of *S. cerevisiae* can tolerate 10 mM putrescine [39], though one of the reports suggests that the strain can tolerate up to 80 mM putrescine without suffering any negative effects [40]. *S. cerevisiae* Y05034 strain was supplied with 100 μ M putrescine in culture medium, with and without proteasome inhibitor MG132 (50 μ M). The concentration of putrescine used in the culture medium was varied from 1 μ M to 1000 μ M in the experiments, where the effect of antizyme on degradation was studied. Cultures of Y651 expressing yEGFP and degron-yEGFP were used as controls for studying the effect of antizyme on degron mediated degradation.

The cultures of Y05034 strain of *S. cerevisiae* expressing the chimeric proteins were incubated with and without cycloheximide to find the reason behind differences in fluorescence intensities of cultures expressing the various fusions of degrons. The cultures were grown in 1 mM putrescine and in the cycloheximide set the antibiotic was added to 4 μ g/ml concentration. Fluorescence intensities of the cultures were monitored and protein concentration was estimated at 30 min intervals. Change in fluorescence intensity per mg protein was calculated and the results were expressed as %. The experiment was repeated in three independent sets.

2.2. Construction of chimeric plasmids

DNA fragments encoding peptides representing the degrons of yODC have been cloned in *Bam*HI and *Sac*I restriction sites of pET30a vector for the purpose of purification and structural studies. For functional characterization, DNA sequences for the degrons of yODC N50, α/β and N α/β were cloned in pUG35 plasmid upstream to yEGFP gene in between *Bam*HI and *Eco*RI restriction sites. Restriction digestions and ligations were done using standard methods [41]. All the constructs were finally

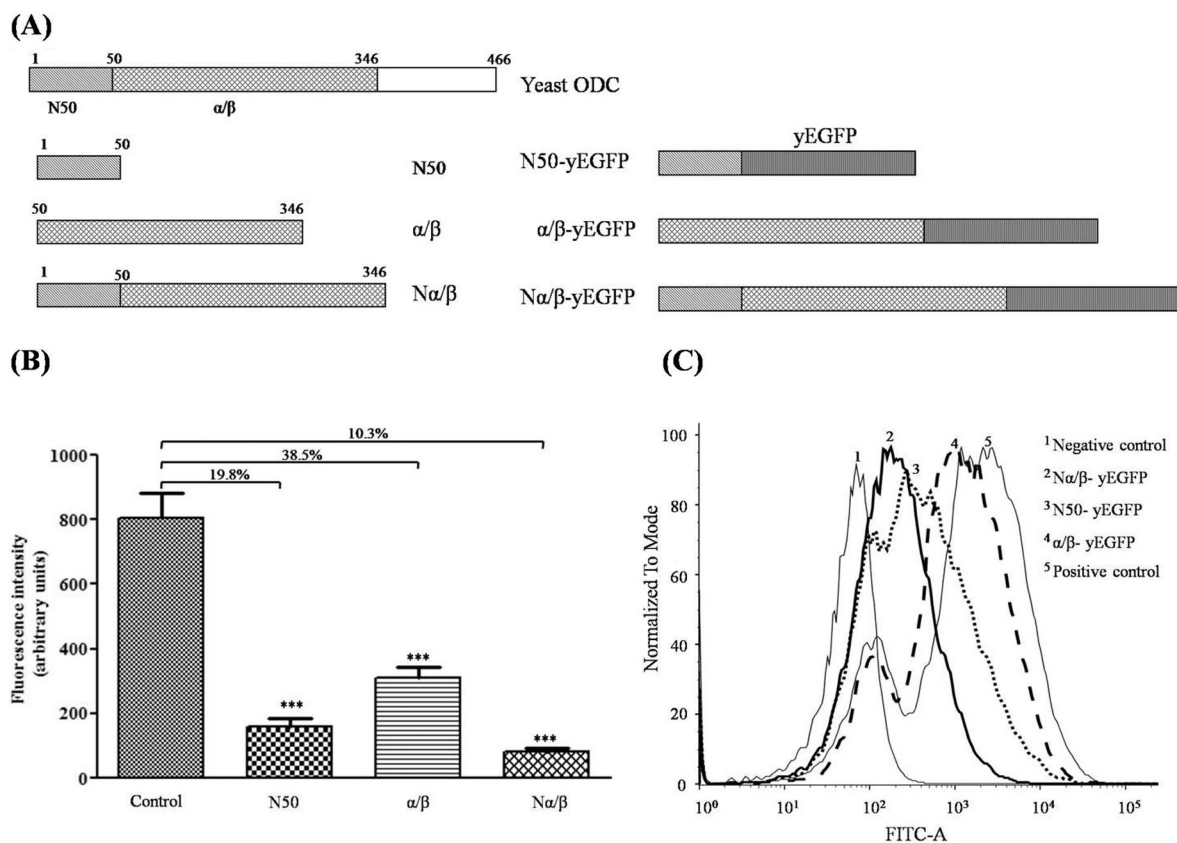


Fig. 1. Yeast ODC (yODC) and deignons of yODC. (A) Pictorial representation of yeast ODC, peptides N50, α/β and $N\alpha/\beta$ (representing deignons of yODC) and their chimeric proteins with yEGFP. (B) Fluorescence was recorded by exciting cells at 488 nm. Emission of yEGFP control and the peptide-yEGFP fusions was recorded at 517 nm. Fluorescence intensities of cultures expressing N50, α/β and $N\alpha/\beta$ peptide sequences in chimeric fusion with yEGFP are 19.8%, 38.5% and 10.3% respectively when compared to control culture expressing yEGFP ($n = 3$ and $***p < 0.001$). (C) Flow cytometric analysis of cells expressing the peptide-yEGFP chimeric proteins and control yEGFP. 1.5×10^4 cells were loaded in flow cytometer and out of them 30,000 events (cells) were analyzed for yEGFP expression with a standard FITC channel (excitation 488 nm, emission 515 nm). The cells expressing N50 (3) and $N\alpha/\beta$ (2) deignons in chimeric fusion with yEGFP show much lower fluorescence due to accelerated degradation of yEGFP than cells expressing α/β (4) fused to yEGFP and only yEGFP control (5). Cells expressing no GFP (1) were used as negative control.

confirmed by DNA sequencing. In the experiments involving β -galactosidase, *KpnI* and *BamHI* were used to digest the vector pUB23 and introduce DNA sequences of deignons. The enzyme β -galactosidase was induced using 2% galactose. The negative control used was ubiquitin- β -galactosidase fusion with methionine as the first residue of β -galactosidase (Ub-Met- β -gal) [42,43], where in the ubiquitin is known to be removed by ubiquitin processing enzymes. Removal of ubiquitin leads to stabilization of the protein.

URA3 gene was introduced into the *EcoRI* site of pUG35 vector. The peptide sequences of yODC deignons N50 and $N\alpha/\beta$ were inserted before the fusion gene for Ura3-yEGFP, making a chimeric construct of deignon-Ura3-yEGFP.

In the yeast expression vector pUb221 the sequence for His-Myc tagged yeast ubiquitin was fused with the DNA fragment for C-terminal of mODC. The resultant vector expressed from *CUP1* promoter the His-Myc-Ub-CmODC fusion, which was used in the present study as a positive control for proteasome mediated degradation.

2.3. Expression and purification of peptides

His-tagged peptides N50, α/β and $N\alpha/\beta$ were over-expressed in *Escherichia coli* BL21 (DE3) cells. Peptide expression was induced with 1 mM isopropyl β -D-1-thiogalactopyranoside (IPTG). The His-tagged peptides were purified by immobilized affinity chromatography by using Ni-NTA agarose resin (Qiagen) according to manufacturer's protocol.

2.4. Circular dichroism

Far UV-CD spectra of the peptides were recorded in the range of 195–250 nm (Jasco-J-815). Other conditions were as described earlier [44–47]. The percentage of secondary structure was calculated with the help of CD Pro software [48] for the peptides N50, α/β and $N\alpha/\beta$.

2.5. Theoretical modeling

AGADIR algorithm was used for predicting the sequence with high α -helical propensity in N50 peptide [49]. The sequences of N50, α/β and $N\alpha/\beta$ were submitted to I-TASSER server for 3D structure prediction [50–52]. The output of I-TASSER was submitted to PyMOL program to view the 3D structure of the peptides [53].

2.6. Fluorescence spectroscopy

Fluorescence intensities of the cultures expressing yEGFP and its chimeric fusions with N50, α/β and $N\alpha/\beta$ were monitored using Hitachi FL-7000 fluorimeter. The cells were excited at 488 nm and fluorescence emission spectra were recorded in the range of 505 to 550 nm. *S. cerevisiae* cultures with no yEGFP were used to normalize autofluorescence of the cells. The experiment was repeated three times in independent sets and the mean values are presented with error bars. SEM values are given in the graph.

2.7. Fluorescence microscopy

Evos Flc fluorescence microscope (Invitrogen) equipped with a green filter was used to observe cells expressing yEGFP and its fusions with N50, α/β and $N\alpha/\beta$.

2.8. Flow cytometry

Fluorescence-activated cell sorting (BD-ariall) was used to quantify yEGFP expression. The instrument settings were as follows: The yeast single-cell population was gated on forward scattering FSC and side scattering SSC. 1.5×10^4 cells were loaded in flow cytometer and out of them 30,000 events (cells) were used to analyze yEGFP expression with a standard FITC channel (excitation 488 nm, emission 515 nm). The raw data was analyzed with FlowJo software by making a histogram plot of the FITC channel.

2.9. Western blot analysis

Western blot analysis of yeast cells expressing only yEGFP and N50, α/β and $N\alpha/\beta$ chimeric fusions of yEGFP were performed as described previously [54] by using rabbit anti-yEGFP monoclonal antibody (1:5000 dilutions, Molecular Probes). Anti-yEGFP antibody was used in the western blot of Ura3-yEGFP control and N50, α/β and $N\alpha/\beta$ chimeric fusions of Ura3-yEGFP. Rabbit anti- β galactosidase antibody (fluorescein isothiocyanate; Novus Biologicals) was used (1:10,000 dilution), in β galactosidase experiment. Purified mouse anti- β actin antibody (BD transduction laboratories) was used at 1:1000 dilution. Anti-c-myc-horse radish peroxidase conjugated antibody (1:1000 diluted) was used for detecting cMyc-Ub-CmODC fusion protein which was used as positive control in the experiment to study the effect of proteasomal inhibitor MG132 on proteasome mediated degradation (Antibody from Roche).

3. Results

3.1. Expression of N50, α/β and $N\alpha/\beta$ as chimeric proteins of yEGFP and monitoring steady state levels of the chimeric fusions

We have cloned the gene fragments encoding the three peptides N50, α/β and $N\alpha/\beta$ as chimeric fusions of yEGFP gene under ADH promoter in the vector pUG35 and expressed them as N50-yEGFP, α/β -yEGFP and $N\alpha/\beta$ -yEGFP in Y05034 strain of *S. cerevisiae* to investigate their potential to act as degrons (Fig. 1A). The strain

Y05034, a derivative of BY4741, is a deletion mutant for *SPE1* gene and requires putrescine supplementation in the culture media for growth since it cannot synthesize polyamines. The fluorescence intensities of yEGFP tagged proteins in the cultures, grown to mid-log phase, were monitored initially to compare their degradation potentials (Fig. 1B). The degron $N\alpha/\beta$ showed highest efficiency in reducing the steady state levels of yEGFP fusion, followed by N50 and α/β . Further, the cultures were examined using flow cytometry and the result was confirmed (Fig. 1C).

3.2. The effect of cycloheximide on the degradation of yEGFP and chimeric yEGFP tagged with N50, α/β and $N\alpha/\beta$

Cycloheximide is an inhibitor of translation in yeast and other eukaryotes. To answer the question of whether the differences seen in the steady state levels of the chimeric fusions of N50, α/β and $N\alpha/\beta$ with yEGFP are due to the differences in their rates of degradation or due to differences in their rates of synthesis, the cultures of Y651 and Y05034 strain of *S. cerevisiae* expressing the chimeric proteins were incubated with and without cycloheximide (Fig. 2A and B). Fluorescence intensity of the cultures was monitored and protein concentration was estimated at 30 minute intervals. Change in fluorescence intensity per mg protein was calculated and the results were expressed as %. The experiment was repeated in three independent sets. In the absence of cycloheximide fluorescence intensity of the culture expressing control yEGFP showed increase with time, while cultures expressing α/β -yEGFP decreased marginally. N50-yEGFP and $N\alpha/\beta$ -yEGFP showed considerable decrease in fluorescence intensity with time. The effect seen in the absence of cycloheximide treatment with N50-yEGFP and $N\alpha/\beta$ -yEGFP, is more pronounced with greater decrease in fluorescence intensity. In the background of inhibition of protein synthesis, the decrease in fluorescence intensity with $N\alpha/\beta$ -yEGFP was more than with N50-yEGFP indicating the greater degradation potential of the degron $N\alpha/\beta$ over N50. In order to have better clarity over the degradation potentials of the constructs we compared the half-lives of control yEGFP, N50-yEGFP, α/β -yEGFP and $N\alpha/\beta$ -yEGFP, under conditions of cycloheximide treatment and antizyme induction in the above experiment. The half-lives of N50-yEGFP and $N\alpha/\beta$ -yEGFP were 86.6 min and 58.9 min respectively. The results were extrapolated to get an approximate estimate of the half-lives of α/β -yEGFP and yEGFP, which were around 3 h and 4 h respectively. Further, the plateau seen with $N\alpha/\beta$ -yEGFP curve between 90 min and 120 min points in the direction of involvement of another protein namely antizyme, the synthesis of which was also negatively influenced by the inhibitor. Cycloheximide

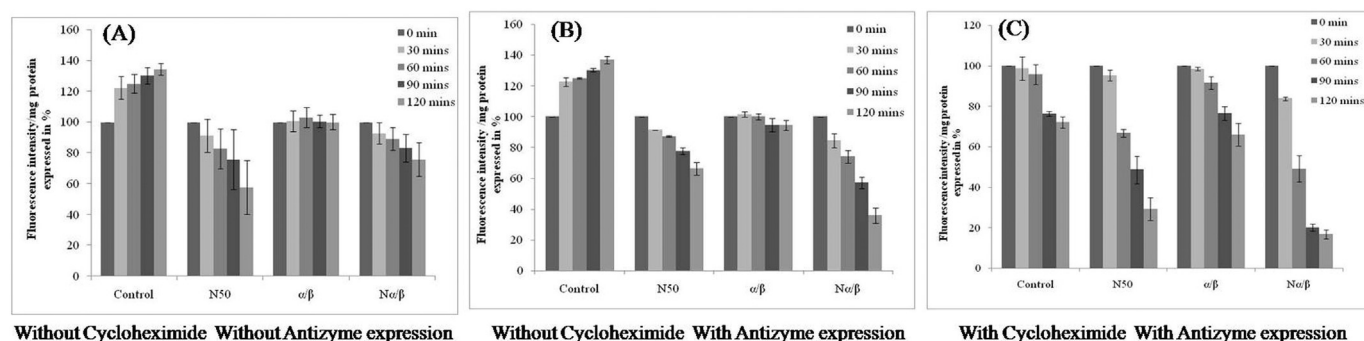


Fig. 2. Degradation of yEGFP tagged with N50, α/β and $N\alpha/\beta$ with time, monitored in the presence and absence of (i) antizyme and (ii) cycloheximide. (i) The cultures of Y651 and Y05034 strains of *S. cerevisiae* expressing N50, α/β and $N\alpha/\beta$ chimeric fusions with yEGFP were monitored for fluorescence at 30 min intervals. Y05034 cells were grown in 1 mM putrescine containing medium. Change in fluorescence intensity per mg protein was determined at 30 minute intervals and the results were expressed as % ($n = 3$) (results with Y651 given in panel 2A and with Y05034 given in panel 2B). $N\alpha/\beta$ -yEGFP showed more degradation with antizyme expression over N50-yEGFP. Control yEGFP and α/β -yEGFP did not show much degradation in the presence and absence of antizyme. (ii) The cultures of Y05034 strains of *S. cerevisiae* expressing N50, α/β and $N\alpha/\beta$ chimeric fusions with yEGFP were grown with and without cycloheximide. Change in fluorescence intensity per mg protein was determined in the presence and absence of cycloheximide and results were presented similar to the above experiment. In the absence of cycloheximide fluorescence intensity of the culture expressing control yEGFP showed increase with time, while cultures expressing N50-yEGFP and $N\alpha/\beta$ -yEGFP showed decrease and α/β -yEGFP showed marginal decrease (panel 2B). With cycloheximide treatment with N50-yEGFP and $N\alpha/\beta$ -yEGFP showed more pronounced decrease in fluorescence intensity. The degradation observed with $N\alpha/\beta$ -yEGFP is more than N50-yEGFP (panel C).

treatment on the other hand produced slight decrease in fluorescence, almost to an equal degree in cells expressing control yEGFP and α/β -yEGFP (Fig. 2B and C).

3.3. The effect of proteasomal inhibitor MG132 on the degradation of yEGFP and chimeric yEGFP tagged with N50, α/β and N α/β

ODC of yeast is rapidly degraded by proteasomes. To test whether the degrons of yODC when grafted on yEGFP are degraded by proteasomes, the log phase cultures of Y05034 strain of *S. cerevisiae* expressing the chimeric proteins were incubated with the proteasomal inhibitor MG132. Fluorescence intensity measurements of the cultures after four hours of exposure to inhibitor showed accumulation of N50-yEGFP and N α/β -yEGFP, while the levels of α/β -yEGFP and yEGFP control remained unchanged (Fig. 3A). Western blot analysis of the same cultures, once again showed increase in intensity of N α/β -yEGFP and N50-yEGFP bands in the lanes containing MG132 treated cultures with respect to untreated samples, whereas MG132 did not show any effect on the intensity of bands of α/β -yEGFP and yEGFP control (Fig. 3B). The results indicate that both N α/β -yEGFP and N50-yEGFP are degraded by proteasomes. However, α/β -yEGFP may not be subject to degradation by proteasomes. The above results were confirmed using fluorescence microscopy (data not shown). The effect of MG132 on the degradation of two more proteins β -galactosidase and Ura3 was tested when they were fused to the degrons N50 and N α/β . Control β -galactosidase remained unaffected both in presence and absence of MG132, whereas degradation of β -galactosidase fusions of N50 and N α/β were inhibited (Fig. 3C). To

have a positive control for our experiments on protein degradation by proteasomes, we have fused the degron from the C-terminal tail of mammalian ODC (CmODC) to N-terminally His-Myc tagged ubiquitin (Ub) and monitored the degradation of His-Myc-Ub-CmODC. In the DNA construct, prior to the fusion of CmODC, the C-terminal glycine of Ub was removed to prevent cleavage of Ub from CmODC. A remarkably stable protein, ubiquitin underwent degradation more rapidly. Addition of proteasomal inhibitor MG132 inhibited degradation of ubiquitin (Fig. 3D). Similarly, control Ura3 remained unaffected by MG132, while degradation of Ura3 fusions of N50 and N α/β were inhibited (Fig. 4D).

3.4. Effect of antizyme on the degradation of proteins yEGFP and Ura3 tagged at the N-terminal with the peptides N50, α/β and N α/β

Increased intracellular pools of polyamines lead to synthesis of the protein antizyme. Antizyme binds monomers of ODC and presents them to proteasomes for degradation, in feedback mechanism of regulation that brings down ODC levels, shutting down polyamine biosynthesis. The two chimeric proteins N α/β -yEGFP and α/β -yEGFP contain antizyme binding element (AzBE) in their sequence. We asked whether AzBE in the peptides N α/β -yEGFP and α/β -yEGFP would successfully be recognized by antizyme for binding. Initially to answer the question, we treated the cultures of Y05034 expressing yEGFP and chimeric yEGFP proteins with increasing concentrations of putrescine and monitored the fluorescence intensity of cultures in mid-log phase (Fig. 4A). Increased polyamine levels caused considerable decrease only in the case of N α/β -yEGFP, establishing that the N α/β sequence in the

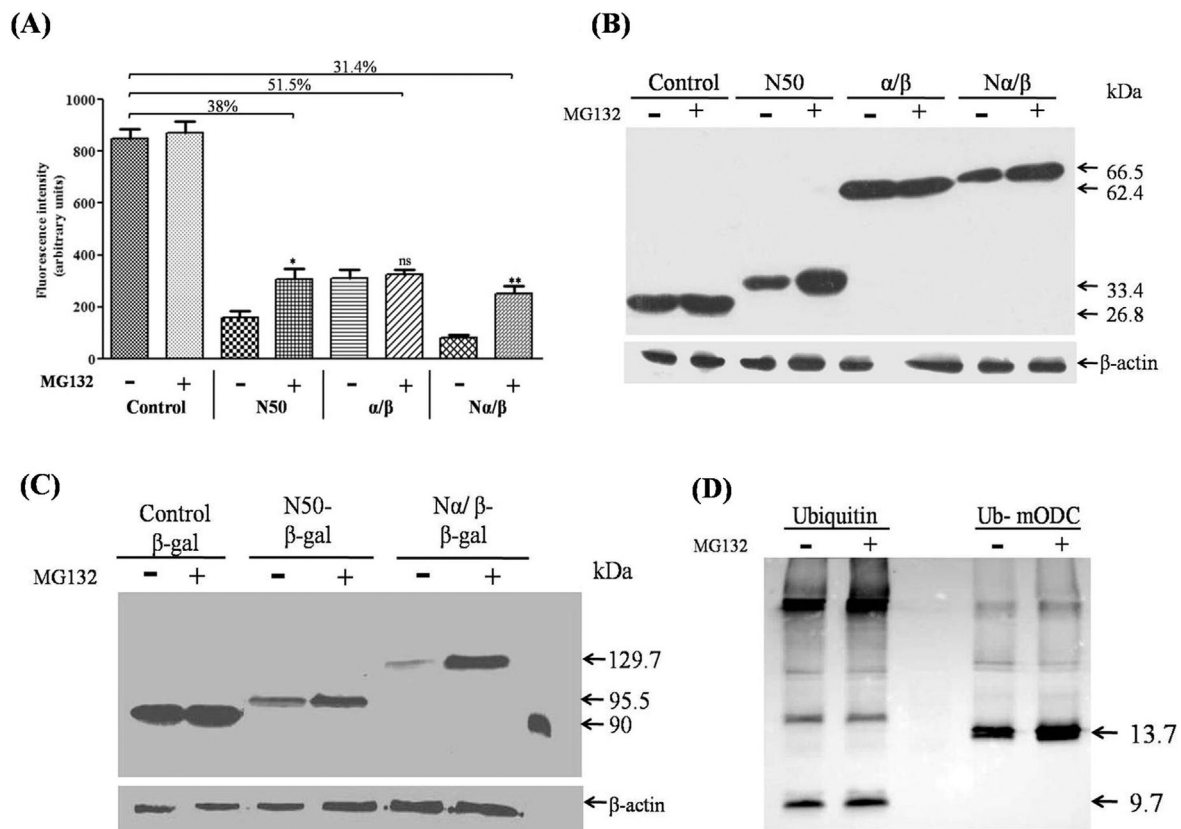


Fig. 3. Effect of MG132 on the degradation of chimeric protein tagged with N50, α/β and N α/β . (A) Cultures of *S. cerevisiae* (Y05034) expressing yEGFP as control and degron-yEGFP chimeric proteins in log phase were subjected to 50 μ M MG132 treatment for 4 h. Their fluorescence intensities were monitored by exciting the cells at 488 nm and recording the emission at 516 nm ($n = 3$ and $*p < 0.01$; $**p < 0.005$, ns – not significant). (B) Western blot analysis of the same samples used for fluorescence studies. Rabbit anti-GFP antibody was used for probing. β -Actin used as load control was probed with anti- β -actin antibody. (C) Western blot analysis of β -galactosidase with N-terminally fused degrons N50 and N α/β showed accumulation of protein with proteasomal inhibitor MG132, establishing that proteasomes are the site of their degradation. Full length β -galactosidase with no fusion was negative control. (D) Ubiquitin is a stable protein. Ubiquitin fused to the C-terminal of mODC (Ub-CmODC) showed accelerated degradation. In the presence of MG132 degradation of Ub-CmODC was inhibited. Ub-CmODC was used as a positive control for the inhibitory effect of MG132 on proteasomes.

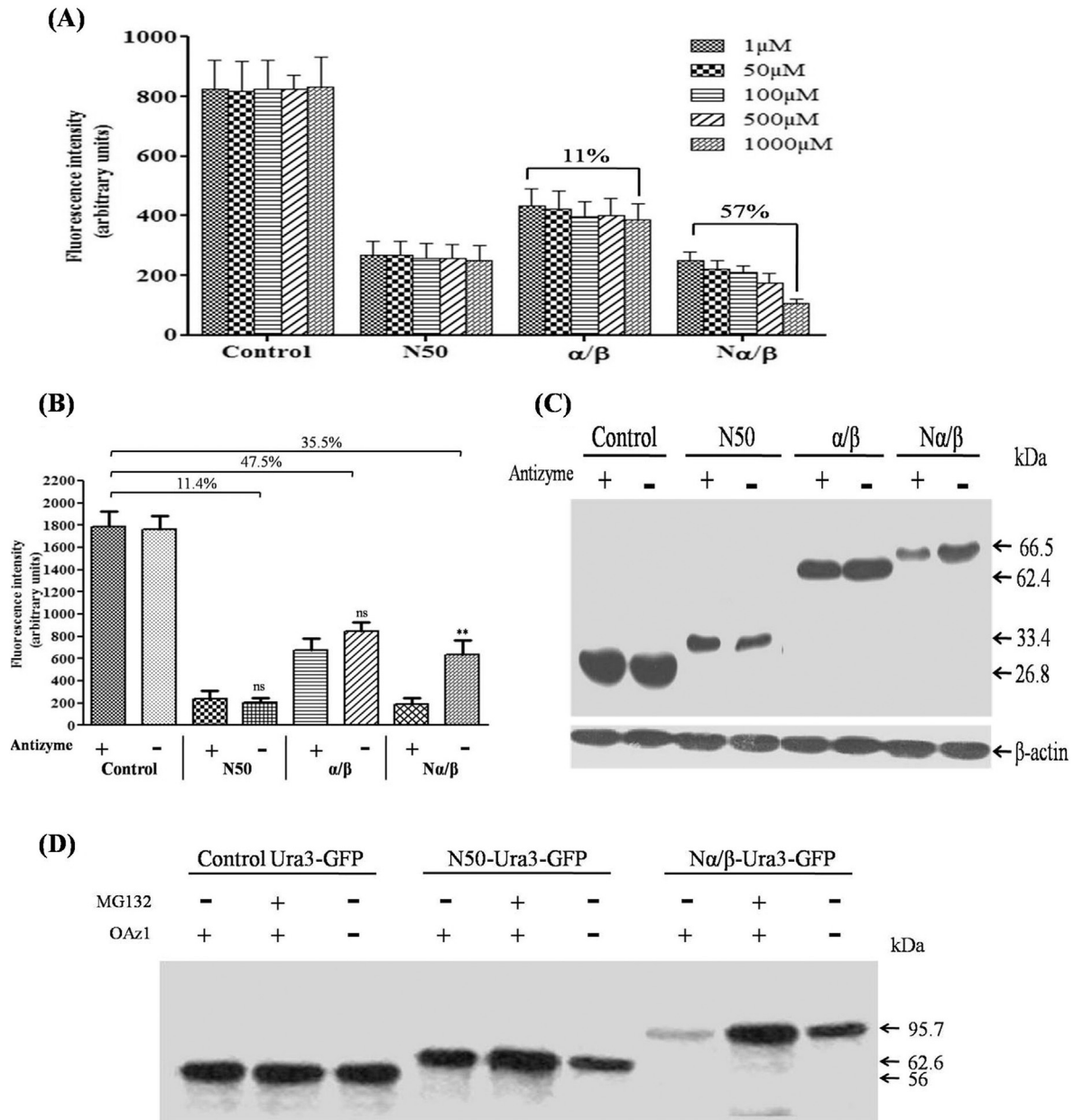


Fig. 4. Effect of antizyme on the degradation of proteins tagged with the peptides N50, α/β and $N\alpha/\beta$. (A) Antizyme expression was induced by varying putrescine concentrations (1 μM to 1000 μM) in culture medium (in B, C and D). Strain Y651 lacking antizyme was used as negative control and Y05034 carrying the gene for antizyme was used as test. (B and C) Fluorescence intensity measurements and western blot analysis of the peptide-yEGFP fusion proteins in the presence (+) and absence (-) of antizyme respectively. For (B) $n = 3$ and $**p < 0.005$, ns – not significant. (C) Anti-GFP antibody was used for western blot analysis. (D) Ura3 fused to yEGFP at C-terminal and degrons N50 and $N\alpha/\beta$ at N-terminal was used to study the effect of antizyme on degradation. In (B, C and D) 1 mM putrescine was added to culture medium. Results indicate better degradation by $N\alpha/\beta$ over N50 in the presence of antizyme induced by 1 mM putrescine.

chimeric protein adopts a conformation that can readily be recognized and bound by antizyme for degradation. However, the slight decrease that was observed in the case of α/β -yEGFP was found to be statistically insignificant. As expected, the yEGFP and N50-yEGFP levels remained unaffected. Putrescine concentrations used in this study are in the range of 1 μM to 1 mM. The strains Y651 and Y05034, which are derivatives of BY4741, can tolerate 1 mM putrescine without suffering any toxic effects of the polyamine.

In order to have a second line of evidence on the contribution of antizyme to targeted degradation, we decided to compare the levels of chimeric proteins in the antizyme deletion strain Y651 to those in Y05034 strain. The results of fluorescence intensity measurements of the cultures (Fig. 4B) and western blots of the cultures (Fig. 4C)

demonstrated that $N\alpha/\beta$ -yEGFP with two degradation signals working in tandem has better degradation potential over the other two degrons. Further, its degradation potential can easily be regulated by varying polyamine levels. The experiment was repeated with N50-Ura3-yEGFP and $N\alpha/\beta$ -Ura3-yEGFP fusion. Ura3-yEGFP fusion was negative control. $N\alpha/\beta$ -Ura3-yEGFP fusion was degraded to a greater degree than N50-Ura3-yEGFP in Y05034 strain, when antizyme was expressed under the influence of putrescine.

To confirm the effect of antizyme induced by putrescine on the degradation rates of degrons, the two strains of yeast Y05034 and Y651 expressing yEGFP and degron-yEGFP fusions were monitored using fluorescence spectroscopy. The cultures of Y05034 were grown in presence of 1 mM putrescine. The experiment was carried out similar

to the cycloheximide experiment and change in fluorescence intensity per mg protein was calculated and the results were expressed as % (Fig. 2A and B).

3.5. Far and near UV CD spectra of the peptides N50, α/β and $N\alpha/\beta$

We wanted to determine if there is any correlation between the degradation efficiency of peptides and their structure. Towards this end, far UV CD spectra were recorded for the peptides N50, α/β and $N\alpha/\beta$ to understand the nature and content of secondary structure (Fig. 5A). The results showed a well formed α/β structure in the case of $N\alpha/\beta$. However, the spectrum of α/β peptide displayed β sheet character as its dominant feature. The degenon character of the N-terminal 44 residues termed as ODS was reported earlier with a conjecture that the N-terminal is unstructured. However, no studies are available on the structure of N-terminal extension and for the first time we took up the structural characterization of N50. Interestingly, the far UV CD spectrum of N50 showed negative ellipticity values at 207 nm and 222 nm. From an earlier study it is known that if the ratio of ellipticities observed at 222 nm and 207 nm corresponds to a value of 0.4, then the structure formed is a 3_{10} helix [55]. With N50 the value observed was 0.418, suggesting the presence of 3_{10} helix. Besides, the analysis of CD spectra using CD Pro indicated the various components of secondary structure in all the three peptides (Table 1).

At this juncture, we addressed the question whether the conformations displayed by these peptides are optimal or there are regions in the peptides which have weak propensity for secondary structure, but are

Table 1

Secondary structural analysis of far-UV CD spectra of the peptides N50, α/β and $N\alpha/\beta$ using CD Pro software.

Reference set: SP43	Helix (%)	Sheet (%)	Turn/unread (%)
$N\alpha/\beta$	30.8	18.6	49.4
α/β	17.7	27.9	54.4
N50	32.3	16.6	50.2

remaining extended under the experimental conditions. With the aim of answering the question, we decided to record the spectra of the degenon peptides in presence of 40% TFE, a solvent known to stabilize α -helical structure in peptides which can form α -helices under ideal conditions, but remain in extended conformations otherwise. From the results presented in Fig. 5B, it is clear that $N\alpha/\beta$ does not show any change in the structure, establishing that its α -helical regions are completely folded and addition of TFE did not have any influence over the secondary structure of the fragment. The α/β fragment showed a change in its secondary structure (Fig. 5C). However, the result observed with N50 was surprising as long stretches of 3_{10} helix are uncommon to proteins in their native state. To test if the above result is a pointer towards α -helical propensity of the peptide, CD spectrum of N50 was recorded in the presence of TFE (2,2,2-trifluoroethanol). The peptide readily adopted α -helical conformation (Fig. 5D).

The near UV CD spectra of the three peptides showed evidence for presence of some tertiary structure (Fig. 6A) which was denatured by the addition of guanidine hydrochloride (Fig. 6B).

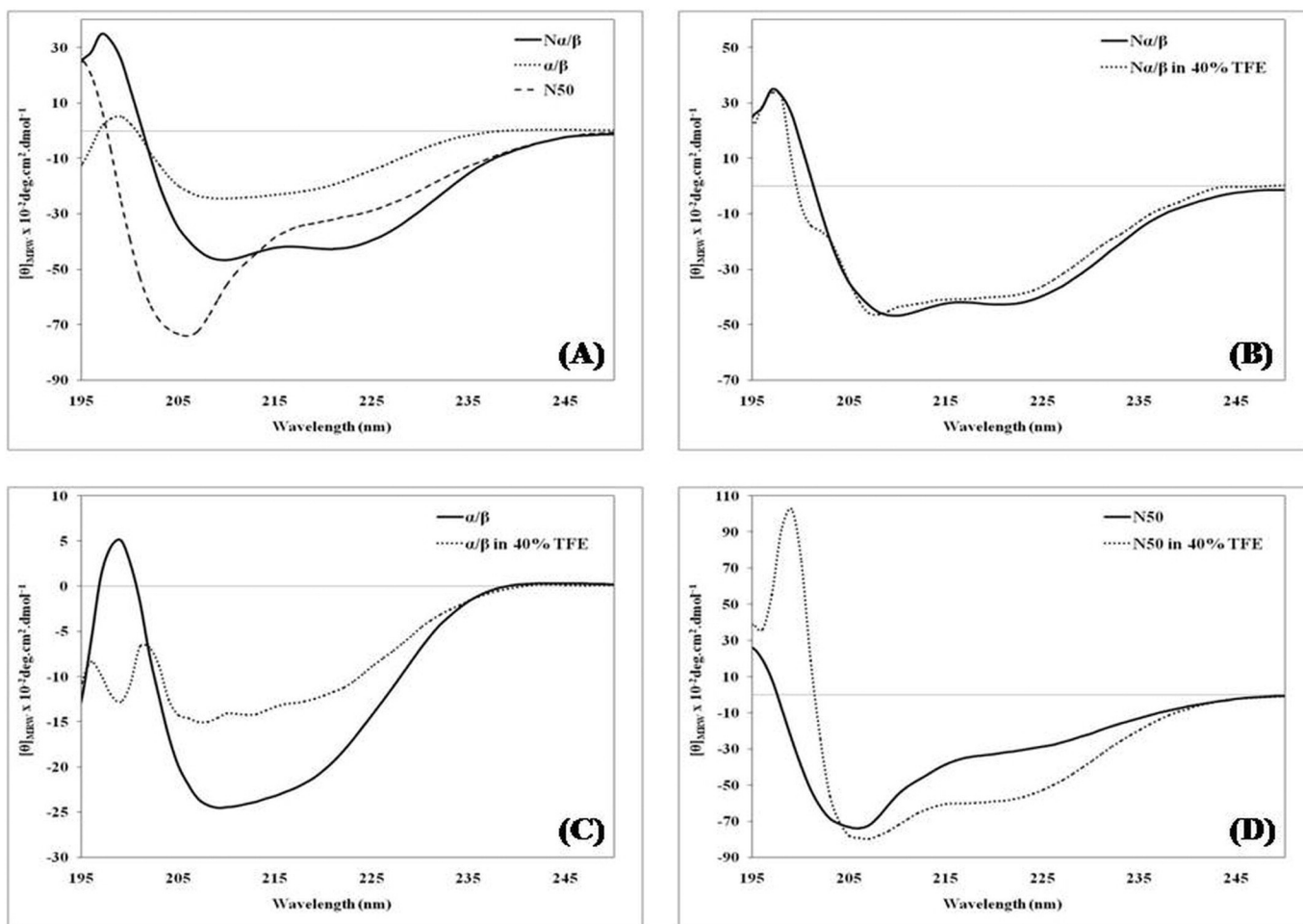


Fig. 5. Far UV CD spectra of (A) the peptides $N\alpha/\beta$, α/β and N50 in 10 mM Tris buffer, pH 8.0, recorded from 195 nm 250 nm to analyze the secondary structure status of the peptides. Far UV CD spectra in buffer (—) and in 40% TFE (····) of the peptides $N\alpha/\beta$ (B), α/β (C) and N50 (D). TFE is known to stabilize helical structure of peptides which cannot form stable helices due to weak propensity for adopting the secondary structure. In (B) $N\alpha/\beta$ does not show any change in the spectrum even after addition of TFE.

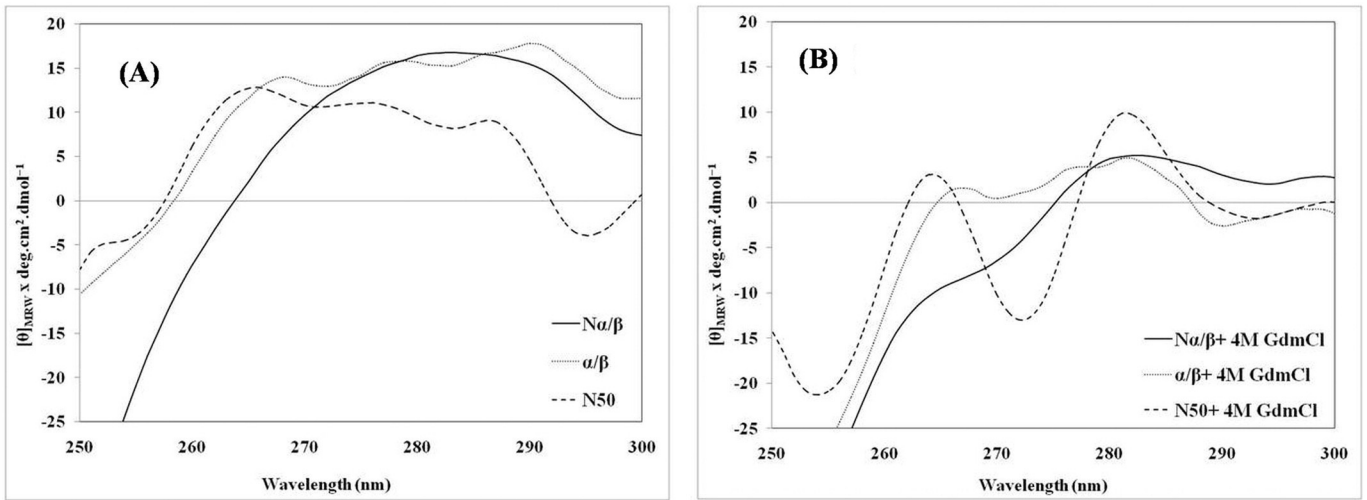


Fig. 6. Near UV CD spectra of the peptides N50, α/β and Nα/β in 10 mM Tris buffer, pH 8.0 (A) and in 4 M guanidine hydrochloride (B).

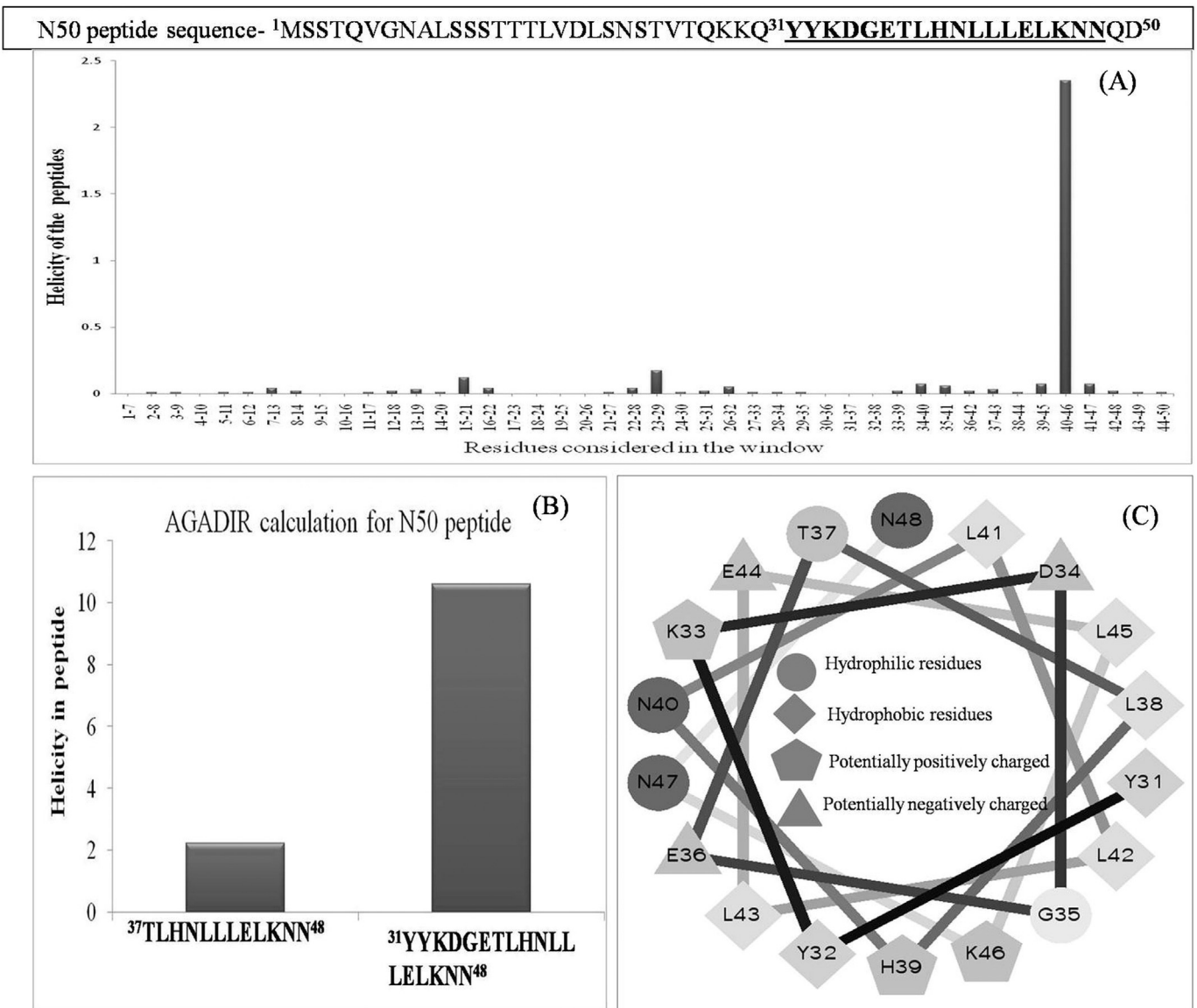


Fig. 7. (A) AGADIR calculations carried out on the entire sequence of N50 sliding a window of 7 residues. (B) The sequences with helical propensity in N50 is shown. (C) Wheel diagram of the peptide ³¹YYKDGETLHNLLLELKNN⁴⁸, showing amphipathic nature.

3.6. Theoretical modeling of N50, α/β and N α/β

When the helical propensity of N50 was evident in far UV CD spectra, to test whether the entire sequence or a part of it takes up helical structure, we have used AGADIR algorithm and the results indicated the sequence ³¹YYKDGETLHNLLELKNN⁴⁸, showed greater preference for helical structure over rest of the peptide sequence (Fig. 7A and B). 3D modeling of the same peptide was carried out on I-TASSER server. The somewhat hyphenated occurrence of hydrophobic and polar residues suggested a possibility of amphipathic α -helix. To check this possibility we have drawn a helical wheel diagram which has supported formation of amphipathic α -helix as a side of the helix has four hydrophobic residues and the other side has polar residues (Fig. 7C).

3D modeling of α/β and N α/β using I-TASSER resulted in TIM like α/β barrel structure. Moreover, with N α/β peptide interactions between regions of N50 and α/β domain were observed (Table 2). The models of the peptides N50, α/β and N α/β generated using Pymol are presented in Fig. 8.

There are differences between the values of secondary structures obtained by CD spectra and 3D modeling. The values observed for various secondary structural features with CD spectra are closer to reality as we have observed them experimentally with the peptides. I-TASSER uses fold recognition to detect structure templates from the protein data bank for a given sequence. The structural fragments so generated are assembled into model of full-length structure. Hence, the 3D model of structure generated indicates structural preference of the sequence rather than the exact content of secondary structure. Since, α/β and N α/β have a large overlap in their sequences, they display almost similar contents of helix and sheet. CD spectrum of α/β has more β -sheet and less α -helix content than N α/β . Besides, addition of TFE made no difference to secondary structure of N α/β , establishing that it has already folded into its optimal and most stable conformation. This observation was also supported by its response to antizyme as seen in the western blots. α/β fragment, in contrast to N α/β has greater β -sheet content and showed a change in secondary structure in TFE, indicating that its α -helix has not folded to its optimal content. Moreover, it could not act as a degron and did not respond to antizyme.

4. Discussion

In the present work, we demonstrate that among the three peptide sequences selected from ODC, two of them namely, peptides N50 and N α/β are effective as degrons. Apparently in both cases the first fifty residues of the N-terminal region lead the chimeric protein successfully into proteasomes for degradation. There was a reduction in the level of degradation observed with N α/β -yEGFP unlike N50-yEGFP in the strain Y651, which lacks antizyme. This could be due to the presence of a compactly folded α/β region downstream to N50, which requires antizyme mediated destabilization or partial unfolding, as a condition prior to the entry of rest of the chimeric protein into proteasome.

Besides, from the results of CD spectra and modeling studies we anticipate interaction between N50 and α/β regions, which may act as a hindrance for degradation N α/β . The interaction of N α/β with antizyme probably introduces a conformational change which loosens the interactions, making N50 region amenable for degradation. The N50 region then extends away from the protein and inserts itself into proteasomal portal once the protein is delivered to proteasome. It appears that the assistance of antizyme is required not only to prevent formation of a dimer by monomers, but also to destabilize the conformation of the N50 region making it amenable to degradation. In the dimeric state the N50 region is most likely buried to avoid degradation. The two degrons which are acting in tandem are responsible for the enhancement of degradation observed with N α/β when compared to N50. The mechanism of degradation of chimeric protein assisted by degrons is presented in Fig. 9.

Another spin off from this study is α/β cannot act as a degron and fails to lead chimeric proteins to proteasome for degradation. At this stage it is difficult to comment on the site of degradation for the chimeric proteins of α/β .

Failure of α/β in targeting the chimeric protein for degradation establishes the importance of N50. At the same time absence of α/β precludes binding to antizyme, depriving the degron of any regulatory mechanism. Hence, even though N50 is an effective degron, it leads the protein towards uncontrolled degradation upsetting the very purpose of targeted degradation. On the other hand the regulatory feature in N α/β makes it an ideal degron.

Hence, among the redesigned degrons N α/β carries many important features: i) it cannot dimerize, as a part of the protein is missing. ii) It is catalytically inactive, a property of great significance in the context of TPD, to obviate polyamine over-expression, and iii) N α/β is an interesting degron with recognition sequence for yeast antizyme. Further, we propose the use of this engineered protein as a tag in mammalian cells, along with yeast antizyme which does not interfere with other mammalian cellular functions [20].

As mentioned earlier the degradation potential of ODS was reported by Godderz et al. in 2011 [36], while the present work was underway. Further the authors made a comment that the peptide is unstructured. ODS which represents the first 44 residues of N-terminal of ODC shares some commonality with the N50 peptide reported here. Structure prediction with the sequence of N50 using I-TASSER and AGADIR algorithm suggested a strong possibility for existence of α -helical conformation between amino acid residues 31 to 48. ODS does not have some of the residues which formed part of α -helix in our model of N50. Furthermore, the interactions observed in our model between first 20 residues of the N-terminal and the α/β domain, seem to play a crucial role in preventing the degradation of ODC at below optimal levels of polyamines. If N-terminal by itself can siphon the monomer to degradation under normal conditions, there would not be any ODC left for polyamine biosynthesis. The conformational change induced in N α/β by antizyme, an indicator of polyamine surplus, activates the otherwise dormant degron N50 in the native protein. Our results of accelerated

Table 2
Polar interactions of N50 region with α/β region in N α/β structure.

Backbone-backbone	Backbone-side chain	Side chain-side chain
Y31-C=O...H-N-G35	H39-C=O...H-N-L43	E57-C=O...H-N-K28
K33-C=O...H-N-T37	N40-C=O...H-N-E44	Q49-C=O...H-O-T121
D34-C=O...H-N-L38	N40-C=O...H-N-L43	K29-N-H...O-T26
G35-C=O...H-N-H39	L41-C=O...H-N-L45	K33-N-H...O=C-E36
E36-C=O...H-N-H39	L42-C=O...H-N-L45	N22-C=O...H-N-N8
E36-C=O...H-N-N40	L42-C=O...H-N-K46	D19-C=O...H-O-S11
T37-C=O...H-N-L41	L43-C=O...H-N-N47	K46-N-H...O=C-D50
L38-C=O...H-N-L42	T14-N-H...O=C-L126	T14-O-H...N(H)-K96
		K28-N-H...O=C-E57
		(2 interactions)
		Q49-C=O...H-O-T121

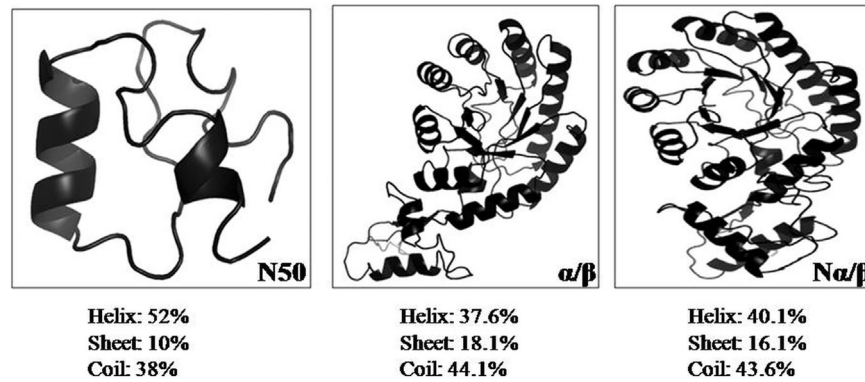


Fig. 8. 3D modeling of peptides representing degrons of yODC on I-TASSER server.

degradation observed with N α/β -yEGFP over N50-yEGFP in the presence of antizyme support this observation.

Our results impart two very distinct and significant roles to N50 region. First, it confirms the earlier observation that it can act as a degnon. Even though α/β fragment could not fold successfully to act as a degnon, presence of N50 helped N α/β fold and act as an antizyme responsive degnon, implicating a role for N50 in the folding of α/β domain.

The work reported by Dohmen's group was elegant and in addition it is pioneering with respect to use of N-terminal peptide of yeast ODC as a degnon. However, our study not only extends the previous work but also adds several novel observations as listed here: (i) we have selected three different peptides for the study and compared their degradation potentials. Studies on the peptides α/β and N α/β were unprecedented. (ii) There were no investigations on the structure of any of these peptides. For the first time our study shows that N α/β can fold by itself into native like conformation and consequently can interact with

antizyme. Further, our results established that α/β cannot adopt native like conformation, providing basis for its functional failure. In spite of carrying the entire sequence representing α/β domain, only one of them is successfully folding into native like conformation is a considerable advance in the structure aspect. (iii) The involvement of N50 in the folding of α/β domain is a surprise find. (iv) N50 does not fold into α -helix in isolation from rest of the sequence. Instead it displays 3_{10} helix like structure. However, far UV CD spectrum of the peptide recorded in TFE establishes that N50 has a potential for adopting α -helical structure and might take up the conformation when it is contiguous with α/β domain. Besides, modeling studies on N50 and N α/β indicated a possibility for interaction between N50 and α/β regions of the protein. Put together these results strongly suggest that these interactions stabilize the structures of both N50 and α/β regions in N α/β and also in native ODC keeping the N-terminal anchored and preventing it from heading for degradation. Interaction between N α/β and antizyme

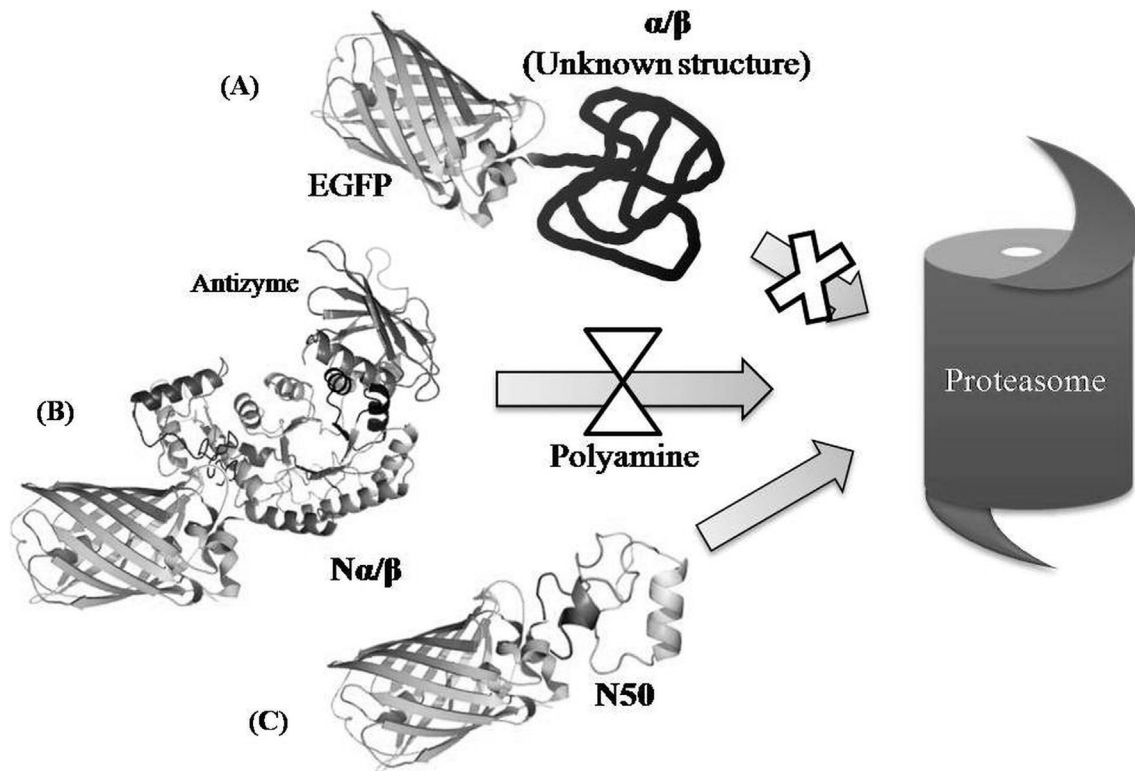


Fig. 9. Proposed mechanism for the degradation of chimeric proteins of yEGFP carrying the peptide tags α/β , N α/β and N50. (A) The peptide tag α/β in spite of carrying antizyme binding sequence AzBE cannot adopt the right structure and fails to act as a degnon. (B) The degnon N α/β carries two degradation signals N50 and AzBE in α/β domain. N α/β acts as an efficient degnon regulated by antizyme, the expression of which is regulated by polyamines. (C) N50 can act as a degnon and since it does not have AzBE its degradation cannot be regulated by antizyme.

or ODC and antizyme leads to a conformational change which is responsible releasing N50 region from the interactions and exposing it for degradation. (v) The construct with $N\alpha/\beta$ undergoes accelerated degradation in response to elevated polyamine concentration. Hence, presence of antizyme binding element provides a handle for modulating the rate of degradation. All these aspects which certainly advance the topic in more than one direction cannot be simply overlooked.

5. Conclusions

In conclusion, this study establishes that in *S. cerevisiae*, the N50 and $N\alpha/\beta$ peptides from ornithine decarboxylase take up secondary structure independent of rest of the protein. They can act as degrons and cause rapid degradation of chimeric proteins. The helical structure adopted by part of N50 most likely facilitates locking up of the region in noncovalent interactions with the adjacent α/β domain in the native protein and in $N\alpha/\beta$ peptide as well, keeping it invulnerable to the otherwise inexorable process of degradation. Hence, chimeric peptide of $N\alpha/\beta$ is more stable compared to chimeric peptide of N50. Besides, α/β domain houses AzBE sequence to interact with antizyme. The enhanced degradation observed with $N\alpha/\beta$ as a consequence of increased expression of antizyme proves that interaction of AzBE sequence in $N\alpha/\beta$ with antizyme induces conformational change in the N-terminal region of the protein, exposing N50 region for degradation. The interaction of AzBE and Antizyme has a very specific role in destabilizing intact yeast ODC by stabilizing monomers and exposing N50 degron. The construct with $N\alpha/\beta$ peptide comes with a built in modulator switch to alter the rates of degradation. The α/β peptide cannot attain α/β structure in the absence of N50 sequence implying that N50 sequence plays a role in the folding of α/β domain. As a consequence of its failure in adopting α/β structure, the peptide also fails to act as a degron. The function of AzBE and antizyme duo becomes redundant, when N50 or α/β domains are dissected out from ODC and grafted on other proteins. Hence, either AzBE or α/β domain cannot be considered as complete and independent degrons. And what is more, the interaction of antizyme with proteasomes is significant for enhancing degradation in a regulated manner, as seen with $N\alpha/\beta$ domain. N50 appears to be important for two entirely distinct reasons, first, as a degron and second, as a region which is essential for the folding of α/β domain.

Acknowledgments

This work was supported by a major research project grant (no. BT/PR939/BRB/10/553/2007) awarded to C. Ratna Prabha from Department of Biotechnology, Ministry of Science and Technology, Government of India. We thank P. Coffino, University of California, Herbert Tabor, National Institutes of Health and Jeffrey Gerst, The Weizmann Institute of Science, Israel for providing us with Y05034 and Y651 strains of *Saccharomyces cerevisiae* and pUG35 plasmid respectively. We thank the DBT-ILSPARE facility of The M. S. University of Baroda, India, for providing us with flow cytometry facility. We thank Prof. Nand Kishore, Department of Chemistry, IIT Bombay, India, for extending circular dichroism facility.

References

- [1] P. Pohjanpelto, E. Holta, O.A. Janne, Mutant strain of Chinese hamster ovary cells with no detectable ornithine decarboxylase activity, *Mol. Cell. Biol.* 5 (1985) 1385–1390.
- [2] C. Steglich, I.E. Scheffler, An ornithine decarboxylase-deficient mutant of Chinese hamster ovary cells, *J. Biol. Chem.* 257 (1982) 4603–4609.
- [3] C.W. Tabor, H. Tabor, Polyamines in microorganisms, *Microbiol. Rev.* 49 (1985) 81–99.
- [4] K. Igarashi, K. Kashiwagi, Polyamine transport in bacteria and yeast, *Biochem. J.* 344 (1999) 633–642.
- [5] K. Igarashi, K. Kashiwagi, Polyamines: mysterious modulators of cellular functions, *Biochem. Biophys. Res. Commun.* 271 (2000) 559–564.
- [6] T. Jakubowicz, B. Wolska-Mitaszko, E. Gasior, T. Kucharzewska, Effect of polyamines on yeast cell-free protein synthesizing system. II. Increase stability of cell-free system in the presence of spermine, *Acta Microbiol. Pol.* 25 (1976) 199–204.
- [7] C.L. Shenvi, K.C. Dong, E.M. Friedman, J.A. Hanson, J.H.D. Cate, Accessibility of 18S RNA in human 40S subunits and 80S ribosomes at physiological magnesium ion concentrations—implications for the study of ribosome dynamics, *RNA* 11 (2005) 1898–1908.
- [8] J.E. Seely, L. Persson, G.J. Sertich, A.E. Pegg, Comparison of ornithine decarboxylase from rat liver, rat hepatoma and mouse kidney, *Biochem. J.* 226 (1985) 577–586.
- [9] D.H. Russell, S.H. Snyder, Amine synthesis in regenerating rat liver: extremely rapid turnover of ornithine decarboxylase, *Mol. Pharmacol.* 5 (1969) 253–262.
- [10] Y. Murakami, S. Matsufuji, T. Kameji, S. Hayashi, K. Igarashi, T. Tamura, K. Tanaka, A. Ichihara, Ornithine decarboxylase is degraded by the 26S proteasome without ubiquitination, *Nature* 360 (1992) 597–599.
- [11] S. Matsufuji, T. Matsufuji, Y. Miyazaki, Y. Murakami, J.F. Atkins, R.F. Gesteland, S. Hayashi, Autoregulatory frameshifting in decoding mammalian ornithine decarboxylase antizyme, *Cell* 80 (1995) 51–60.
- [12] Z. Bercovich, Y. Rosenberg-Hasson, A. Ciechanover, C. Kahana, Degradation of ornithine decarboxylase in reticulocyte lysate is ATP-dependent but ubiquitin-independent, *J. Biol. Chem.* 264 (1989) 15949–15952.
- [13] Y. Rosenberg-Hasson, Z. Bercovich, A. Ciechanover, C. Kahana, Degradation of ornithine decarboxylase in mammalian cells is ATP dependent but ubiquitin independent, *Eur. J. Biochem.* 185 (1989) 469–474.
- [14] J.R. Glass, E.W. Gerner, Spermidine mediates degradation of ornithine decarboxylase by a non-lysosomal, ubiquitin-independent mechanism, *J. Cell. Physiol.* 130 (1987) 133–141.
- [15] S. Gandre, C. Kahana, Degradation of ornithine decarboxylase in *Saccharomyces cerevisiae* is ubiquitin independent, *Biochem. Biophys. Res. Commun.* 293 (2002) 139–144.
- [16] M.K. Chattopadhyay, C. Fernandez, D. Sharma, P. McPhie, D.C. Masion, Yeast ornithine decarboxylase and antizyme form a 1:1 complex in vitro: purification and characterization of the inhibitory complex, *Biochem. Biophys. Res. Commun.* 406 (2011) 177–182.
- [17] S. Matsufuji, T. Matsufuji, Y. Miyazaki, Y. Murakami, J.F. Atkins, R.F. Gesteland, S-I Hayashi, Autoregulatory frameshifting in decoding mammalian ornithine decarboxylase antizyme, *Cell* 80 (1995) 51–60.
- [18] I.P. Ivanov, R.F. Gesteland, J.F. Atkins, Evolutionary specialization of recoding: frameshifting in the expression of *S. cerevisiae* antizyme mRNA is via an atypical antizyme shift site but is still +1, *RNA* 12 (2006) 332–337.
- [19] S. Gandre, Z. Bercovich, C. Kahana, Ornithine decarboxylase-antizyme is rapidly degraded through a mechanism that requires functional ubiquitin-dependent proteolytic activity, *Eur. J. Biochem.* 269 (2002) 1316–1322.
- [20] Z. Porat, G. Landau, Z. Bercovich, D. Krutauz, M. Glickman, C. Kahana, Yeast antizyme mediates degradation of yeast ornithine decarboxylase by yeast but not by mammalian proteasome: new insights on yeast antizyme, *J. Biol. Chem.* 283 (2008) 4528–4534.
- [21] J.J. Almrud, M.A. Oliveira, A.D. Kern, N.V. Grishin, M.A. Phillips, M.L. Hackert, Crystal structure of human ornithine decarboxylase at 2.1 Å resolution: structural insights to antizyme binding, *J. Mol. Biol.* 295 (2000) 7–16.
- [22] A.D. Kern, M.A. Oliveira, P. Coffino, M.L. Hackert, Structure of mammalian ornithine decarboxylase at 1.6 Å resolution: stereochemical implications of PLP-dependent amino acid decarboxylases, *Structure* 7 (1999) 567–581.
- [23] W.A. Fonzi, P.S. Sypher, The gene and the primary structure of ornithine decarboxylase from *Saccharomyces cerevisiae*, *J. Biol. Chem.* 262 (1987) 10127–10133.
- [24] M. Zhang, A.I. MacDonald, M.A. Hoyt, P. Coffino, Proteasomes begin ornithine decarboxylase digestion at the C terminus, *J. Biol. Chem.* 279 (2004) 20959–20965.
- [25] M. Zhang, C.M. Pickart, P. Coffino, Determinants of proteasome recognition of ornithine decarboxylase, a ubiquitin-independent substrate, *EMBO J.* 22 (2003) 1488–1496.
- [26] M.A. Hoyt, M. Zhang, P. Coffino, Ubiquitin independent mechanisms of mouse ornithine decarboxylase degradation are conserved between mammalian and fungal cells, *J. Biol. Chem.* 278 (2003) 12135–12143.
- [27] Y. Miyazaki, S. Matsufuji, Y. Murakami, S. Hayashi, Single amino-acid replacement is responsible for the stabilization of ornithine decarboxylase in HMOA cells, *Eur. J. Biochem.* 214 (1993) 837–844.
- [28] R.A. DeScenzo, S.C. Minocha, Modulation of cellular polyamines in tobacco by transfer and expression of mouse ornithine decarboxylase cDNA, *Plant Mol. Biol.* 22 (1993) 113–127.
- [29] C.R. Prabha, S. Mukherjee, R. Raman, S. Kulkarni, The ends and means of artificially induced targeted protein degradation, *Appl. Microbiol. Biotechnol.* 96 (2012) 1111–1123.
- [30] A. Varshavsky, The N-end rule: functions, mysteries, uses, *Proc. Natl. Acad. Sci. U. S. A.* 93 (1996) 12142–12149.
- [31] S. Rogers, R. Wells, M. Rechsteiner, Amino acid sequences common to rapidly degraded proteins: the PEST hypothesis, *Science* 234 (1986) 364–368.
- [32] P. Loetscher, G. Pratt, M. Rechsteiner, The C terminus of mouse ornithine decarboxylase confers rapid degradation on dihydrofolate reductase. Support for the pest hypothesis, *J. Biol. Chem.* 266 (1991) 11213–11220.
- [33] M. Jungbluth, C. Renicke, C. Taxis, Targeted protein depletion in *Saccharomyces cerevisiae* by activation of a bidirectional degron, *BMC Syst. Biol.* 4 (2010) 176, <http://dx.doi.org/10.1186/1752-0509-4-176>.
- [34] C. Renicke, D. Schuster, S. Usherenko, L.-O. Essen, C. Taxis, A LOV2 domain based optogenetic tool to control protein degradation and cellular function, *Chem. Biol.* 20 (2013) 619–626.
- [35] S. Matsuzawa, M. Cuddy, T. Fukushima, J.C. Reed, Method for targeting protein destruction by using a ubiquitin-independent, proteasome-mediated degradation pathway, *Proc. Natl. Acad. Sci. U. S. A.* 102 (2005) 14982–14987.

- [36] D. Godderz, E. Schafer, R. Palanimurugan, R.J. Dohmen, The N-terminal unstructured domain of yeast ODC functions as a transplantable and replaceable ubiquitin-independent degron, *J. Mol. Biol.* 407 (2011) 354–367.
- [37] C.R. Prabha, P. Mishra, M. Shahukar, Isolation of a dosage dependent lethal mutation in ubiquitin gene of *Saccharomyces cerevisiae*, *Macromol. Symp.* 287 (2010) 89–94.
- [38] M. Sharma, C.R. Prabha, Construction and functional characterizations of double and triple mutants of paralla β -bulge of ubiquitin, *Indian J. Exp. Biol.* 49 (2011) 919–924.
- [39] M.C. Teixeira, T.R. Cabrito, Z.M. Hanif, R.C. Vargas, S. Tenreiro, I. Sa-Correia, Yeast response and tolerance to polyamine toxicity involving the drug: H⁺ antiporter Qdr3 and the transcription factors Yap1 and Gcn4, *Microbiology* 157 (2011) 945–956.
- [40] K. Tachihara, T. Uemura, K. Kashiwagi, K. Igarashi, Excretion of putrescine and spermidine by the protein encoded by YKL174c (TPO5) in *Saccharomyces cerevisiae*, *J. Biol. Chem.* 280 (2005) 12637–12642.
- [41] J. Sambrook, E.F. Fritsch, T. Maniatis, *Molecular Cloning: A Laboratory Manual*, 2 ed. Cold Spring Harbor Laboratory Press, Cold Spring Harbor, NY, 1989.
- [42] A. Bachmair, D. Finley, A. Varshavsky, In vivo half-life of a protein is a function of its amino-terminal residue, *Science* 234 (1986) 179–186.
- [43] R.T. Baker, P.G. Board, The human ubiquitin-52 amino acid fusion protein gene shares several structural features with mammalian ribosomal protein genes, *Nucleic Acids Res.* 19 (1991) 1035–1040.
- [44] C. Ratnaprabha, Y.U. Sasidhar, Conformational features of disulfide intact and reduced forms of hen egg white lysozyme in aqueous solution in the presence of trifluoroethanol (TFE): implications for protein folding intermediates, *J. Chem. Soc. Faraday Trans.* 94 (1998) 3631–3637.
- [45] P. Mishra, C.R. Prabha, C.M. Rao, S. Volety, Q2N and S65D substitutions of ubiquitin unravel functional significance of the invariant residues Gln2 and Ser65, *Cell Biochem. Biophys.* 61 (2011) 619–628.
- [46] P. Mishra, S. Volety, C.M. Rao, C.R. Prabha, Glutamate64 to glycine substitution in G1 beta-bulge of ubiquitin impairs function and stabilizes structure of the protein, *J. Biochem.* 146 (2009) 563–569.
- [47] Y.U. Sasidhar, C.R. Prabha, Conformational features of reduced and disulfide intact forms of hen egg white lysozyme in aqueous solution in presence of 3-chloro-1, 2-propanediol and dioxane: implications for protein folding intermediates, *Indian J. Biochem. Biophys.* 37 (2000) 97–106.
- [48] N. Sreerama, R.W. Woody, Estimation of protein secondary structure from circular dichroism spectra: comparison of CONTIN SELCON, and CDSSTR methods with an expanded reference set, *Anal. Biochem.* 287 (2000) 252–260.
- [49] V. Munoz, L. Serrano, Elucidating the folding problem of helical peptides using empirical parameters, *Nat. Struct. Biol.* 1 (1994) 399–409.
- [50] A. Roy, A. Kucukural, Y. Zhang, I-TASSER: a unified platform for automated protein structure and function prediction, *Nat. Protoc.* 5 (2010) 725–738.
- [51] J. Yang, R. Yan, A. Roy, D. Xu, J. Poisson, Y. Zhang, The I-TASSER Suite: protein structure and function prediction, *Nat. Methods* 12 (2015) 7–8.
- [52] Y. Zhang, I-TASSER server for protein 3D structure prediction, *BMC Bioinf.* 9 (2008) 40.
- [53] W.L. Delano, *The PyMOL Molecular Graphics System*, DeLano Scientific, San Carlos, CA, USA, 2002 (Available from: <http://www.pymol.org>).
- [54] A. Doshi, P. Mishra, M. Sharma, C.R. Prabha, Functional characterization of dosage-dependent lethal mutation of ubiquitin in *Saccharomyces cerevisiae*, *FEMS Yeast Res.* 14 (2014) 1080–1089.
- [55] M.C. Manning, R.W. Woody, Theoretical CD studies of polypeptide helices: examination of important electronic and geometric factors, *Biopolymers* 31 (1991) 569–586.